

***RRR*-Measurement Techniques on High Purity Niobium**

W. Singer, A. Ermakov, X. Singer

1. Introduction

It is well-known that, among of all pure metals, niobium, with its high critical temperature and critical magnetic field, is the favourite material for the fabrication of superconducting RF cavities. Niobium is chemically inert (at room temperature the surface is covered by a protecting oxide layer), it can be machined, deep drawn, welded and it is available as bulk and sheet material in any size.

For good performance of superconducting RF cavities a high thermal conductivity in the cavity wall is required (at least 10 W/m·K at 2K) to guide the dissipated radio frequency (RF) power to the liquid helium coolant. For bulk niobium cavities this demands niobium of high purity.

The residual resistivity ratio ($RRR=300$ for a high gradient cavity) is a common indicator of the level of purity. The main interstitially dissolved impurities, oxygen, nitrogen, hydrogen and carbon (O, N, H, C), act as scattering centers for unpaired electrons and reduce the RRR . Oxygen is dominant due to its high affinity to Nb. The influence of hydrogen on the RRR is not so significant, but the content of hydrogen should be kept small (less than 3-5 $\mu\text{g/g}$) to prevent hydride precipitation and degradation of the Q-value of the high RRR cavities under certain cool-down conditions (hydrogen Q decrease).

Among the substitutionally dissolved metallic impurities, tantalum has the highest concentration. This element accompanies niobium in most ores. Modern separating methods are based on solvent extraction and easily allow the attainment of an impurity level below 500 $\mu\text{g/g}$, which is normally harmless for the cavity performance. Next in abundance among substitutional impurities are metals such as tungsten, titanium, molybdenum, iron and nickel usually at a level less than 30-50 $\mu\text{g/g}$.

The phonon contribution of thermal conductivity is very strongly influenced by dislocations [1]. The operating temperature of the superconducting cavities in most cases is found above the temperature at which the influence of the phonon contribution is significant, so the main interest is to improve electron conductivity thereby reducing the concentration of interstitial impurities. If the phonon contribution is negligible, the RRR is approximately proportional to thermal conductivity. A simplified relationship between the thermal conductivity and RRR at 4.2 K is known [2, 3].

$$\lambda = \frac{RRR}{4} \Big|_{T=4.2K} \quad (1)$$

High RRR values are indicating high material purity for recrystallized material even if a direct estimate of the individual impurities' impact via electron scattering is not possible. Most laboratories and companies working with high purity niobium use RRR as the first criterion of the level of purity, which can be measured easier and faster compared to thermal conductivity. At the same time there are some discrepancies in the definition of RRR of niobium, in particular because of its superconducting behavior at low temperatures. Applying different methods of RRR measurement at different laboratories sometimes produces problems for data comparison and evaluation and causes debates in the SRF community. In order to support a unified understanding of RRR usage and meaning in the community, the

RRR measurement methods and the boundary conditions for interpretation are summarized in the present paper. This overview is based on tests and experimental data collected at DESY over the last 15 years.

2. Definition of *RRR*

As well-known from the electron theory of metals [4], in general cases the electrical resistivity of metals (Mathiessen's rule) at low temperature can be described as [5, 6]

$$\rho = \rho_{res} + \rho_{ph}(T) + \rho_m \quad (2)$$

where the first term is the residual resistivity at $T \sim 0\text{K}$ caused mainly by electron-impurity scattering and scattering on lattice defects ($\rho_{res} = \rho_{imp} + \rho_{def}$); the second term in equation 2 represents the temperature dependent electron-phonon scattering and ρ_m is the resistivity term in a magnetic field.

Scattering of conduction electrons on the lattice (phonon scattering) is absent at $T=0\text{K}$ due to the zero fluctuations of the atoms in the lattice. The ρ_{def} term plays an important role for work-hardened niobium and can reduce the *RRR* up to a factor of two. For recrystallized niobium the ρ_{def} contribution is small. In this case the total resistivity described by equation (2) in the absence of a magnetic field consists only of electron-impurity scattering and electron-phonon scattering contributions.

Resistivity caused by scattering of conduction electrons on homogeneously distributed "chemical" defects (foreign atoms) is proportional to their concentration. The influence of the most important impurity atoms such as O, H, N, C, Ta, Zr etc. on electron-impurity scattering is analyzed in some of the reference works [7, 8]. The most popular is the data of [9] determined on the basis of resistance measurements on niobium voluntarily contaminated by impurities.

$$\rho = \rho_{ph}(T) + \sum \frac{\Delta\rho_i}{\Delta C_i} C_i \quad (3)$$

The resistance coefficients $\frac{\Delta\rho_i}{\Delta C_i}$ are given in Table 1.

TABLE 1. Residual Resistance Coefficients of different atoms as found by K. K. Schulze [9]

Impurity atoms	O	H	N	C	Ta	Zr
$\Delta\rho_i/\Delta C_i, 10^{-10}$ ohm-cm/at.-ppm	4,5	0,8	5,2	4,3	0,25	0,6-1,4

In absolutely pure metals having a lattice without structural defects at temperatures close to 0 K, resistivity tends to be zero (as shown in Fig. 1).

The *RRR* is defined as the ratio:

$$RRR = \frac{\rho(300K)}{\rho(4.2K)} \quad (4)$$

where $\rho(300\text{ K})$ and $\rho(4.2\text{ K})$ are the resistivity of Nb at room and liquid helium temperatures, respectively, at standard atmospheric pressure [10]. With the superconducting behaviour of Nb (below $T_C=9.3\text{ K}$), $\rho(4.2\text{ K})=0$ has to be taken into account for *RRR* determination.

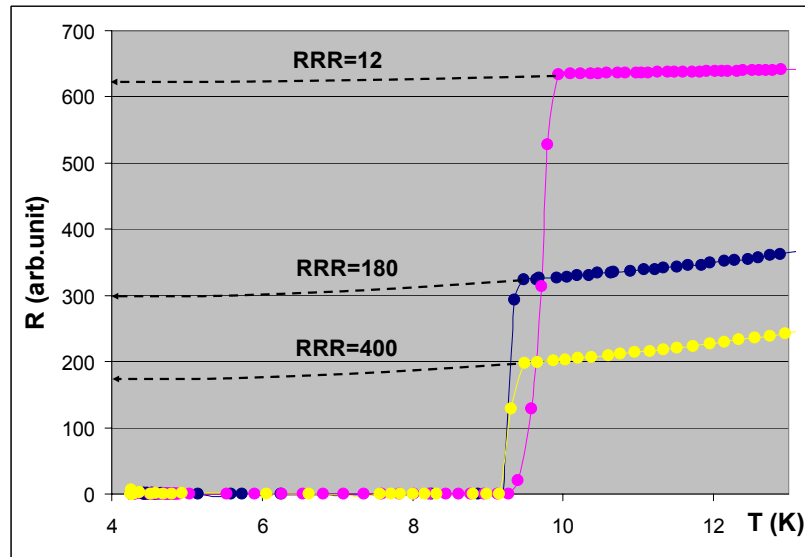


FIG. 1. Typical $\rho(T)$ curves for Nb samples of different purity

Therefore in the practical implementation several special approaches lead to several different methods to obtain the RRR of Nb.

1. DC-method for RRR determination at T_C (in the case of Nb $T_C \sim 9.3$ K). For example $RRR = R_{300K} / R_{10K}$ [7, 11, 12].
2. DC-method for RRR determination by extrapolation of $\rho(T)$ curve to 4.2 K. [13, 14]
3. DC-method for RRR determination by suppressing the Nb superconducting behavior with a magnetic field and extrapolation of $\rho(B)$ curve at $T=4.2$ K to the zero magnetic field B [10, 13]
4. AC-eddy current method as a nondestructive method performed directly on the cavity surface [15]
5. AC-inductive method for RRR determination [16]

3. DC-method – general remarks

In DC-methods the resistivity is obtained by a standard 4-point measurement. The average size of the samples in cross section is normally in the range of 1-15 mm² and 30-100 mm in length. The warm-up and cool-down procedure usually is performed by immersing the sample into liquid helium. The temperature is mainly controlled by Cernox temperature sensors. With a 4-point method, one set of conductors drives the current I through the sample and the second set of conductors picks up the voltage U (Fig. 2). Some current may flow through the voltage but can be ignored since it normally is sufficiently small. In most cases a current in the range of 1-3 A is applied.

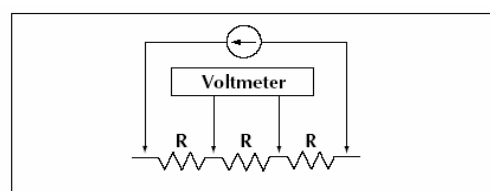
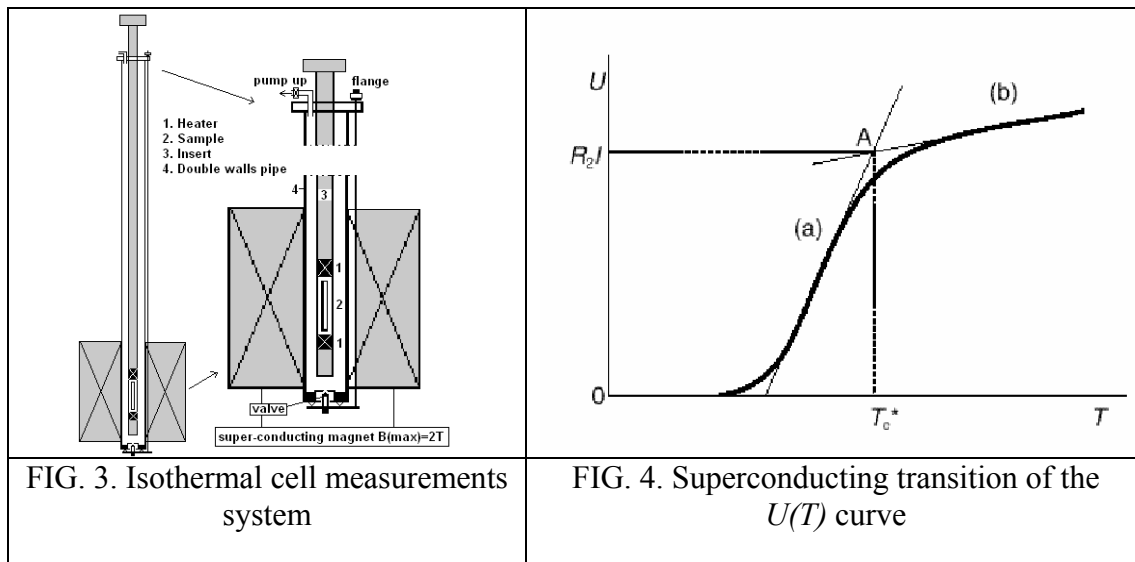


FIG. 2. Scheme of 4-point method

The voltage produced at the junctions of dissimilar metals can impact the measurement accuracy and has to be kept at small levels. The thermoelectric voltage that appears due to the gradient of the temperature along the sample can play an important role. Thus the temperature gradient has to be kept small. In addition this thermal voltage can be subtracted from the measured signal. For example, a current reversal method is applied at DESY to avoid this problem. The thermal voltage is measured by currents of opposite directions. The two measurements are then combined to cancel the effect of thermoelectric voltage.

The homogeneous temperature distribution in a sample during the measurements can be achieved using a special isothermal cell (Fig. 3). This isothermal cell consists of a stainless steel pipe with double walls with vacuum between the walls. For quick cool-down of the sample from room temperature to $T \sim 4.2$ K, a valve on the bottom of the working cell is installed allowing entrance of a gas into the previously evacuated cell. The temperature dependencies of resistivity are measured by slowly heating the sample clamped on the copper fixture with heaters mounted on it (Fig. 3). The deviations of the temperature during heating up or cool-down of the sample are very small, thus allowing precise determination of the point of superconducting jump.



3.1. DC-method: RRR determination at $T_C \sim 9.3$ K

The creation of Cooper pairs and absence of DC resistivity of niobium below T_C is the reason for different approaches in RRR definition and measurement principles. The easiest method consists of measuring the sample's resistivity above T_C and very close to it. The residual resistivity at point A (Fig. 4), which is an intersection of two lines matching sections (a) and (b), is recorded. Taking into account that $\rho = U/I$, RRR is determined by

$$RRR = \frac{U(300K)}{U(9.3K)} \quad (5)$$

Some laboratories and companies [7, 11, 12] are using this method.

Accuracy estimation: The accuracy of RRR measurements depends significantly on the accuracy in determining the intersection A (Fig. 4). Systematic errors appeared due to the measurement of temperature and voltage drop and reproducibility of sample fixing. Quantitatively the accuracy can be estimated using DESY parameters. The voltage drop measured by the Keithley Digital-Multimeter 2001 with pre-amp is

in the range of 2 mV with a systematic error of about 1 nV (less than 1% of the total voltage magnitude). The current provided is constant, so instability of the applied current through the sample is very low, about 1mA (relative error is 0.1%). The total accuracy (systematic and absolute accuracy) of RRR measurements including assembling and disassembling the sample is in the range 2-3%.

The advantage of this method is its simplicity. However, most scientific laboratories use the common RRR definition (Eq. 4). The RRR value evaluated at T_C is approx. 8-10% smaller compared to the standard evaluation of RRR at 4.2K, which can create misunderstanding in data comparison.

3.2. DC-method: RRR determination by extrapolation of $\rho(T)$ curve

As it was shown above the normal state electrical resistivity $\rho(T)$ can be considered as a composition of the residual resistivity ρ_{res} and temperature dependent phonon contribution (some times called ideal resistivity $\rho_{ideal}(T)$):

$$\rho(T) = \rho_{res} + \rho_{ideal}(T) \quad (6)$$

ρ_{res} is essentially independent of temperature for $T < T_{Fermi}$ [$T_{Fermi} = E_{Fermi}/k$, where E_{Fermi} is the chemical potential of the system]. For niobium $T_{Fermi} = 1.1 \times 10^5 K$. For most Nb samples, $\rho_{res} \gg \rho_{ideal}(T)$ at $T \leq 10K$; only for very pure samples, with impurity content smaller than 1^{-10} at. ppm (parts per million (atomic)), $\rho_{ideal}(T)$ will be comparable to ρ_{res} . Berthel and Webb [17, 23] measured the temperature dependent fraction $\rho_{ideal}(T)$ of single crystalline high purity niobium samples ($RRR \approx 16500$) and matched it on the basis of the theoretically expected functional dependency [17, 23]:

$$\frac{\rho_{id}(T)}{\rho_{id}(300K)} = aT^2 + bT^3 \int_0^{\Theta/T} \frac{x^3}{(e^x - 1)(1 - e^{-x})} dx + cT^5 \int_0^{\Theta/T} \frac{x^5}{(e^x - 1)(1 - e^{-x})} dx \quad (7)$$

At a temperature above T_C , but very close to it, the temperature dependent fraction to the resistivity $\rho_{ideal}(T)$ cannot be neglected; it has to be extracted with the help of equation (7).

$$RRR = \frac{\rho(300K)}{\rho(T_{meas}) - \rho_{ideal}(T_{meas}) + \rho_{ideal}(4.2K)} \quad (8)$$

If we consider that $\rho(300K) \approx \rho_{ideal}(300K) \approx \frac{U(300K)}{I}$, then RRR will be expressed as

$$RRR = \frac{U(300K)}{U(T_{meas}) - U_{ideal}(300K) \frac{(\rho_{ideal}(T_{meas}) - \rho_{ideal}(4.2K))}{\rho(300K)}} \quad (9)$$

According to the references [17, 23],

$$\frac{\rho_{ideal}(9.3K)}{\rho_{ideal}(300K)} - \frac{\rho_{ideal}(4.2K)}{\rho_{ideal}(300K)} = 2.1587 \times 10^{-4} \quad (10)$$

Then, the formula for RRR estimation used at DESY is as follows:

$$RRR = \frac{U(300K)}{U(9.3K) - U(300K) \times 2.1587 \times 10^{-4}} \quad (11)$$

The implementation of this method has the purpose of obtaining the U value at the intersection – (red point in Fig. 5) on the $U(T)$ curve and calculating the RRR using equation (11).

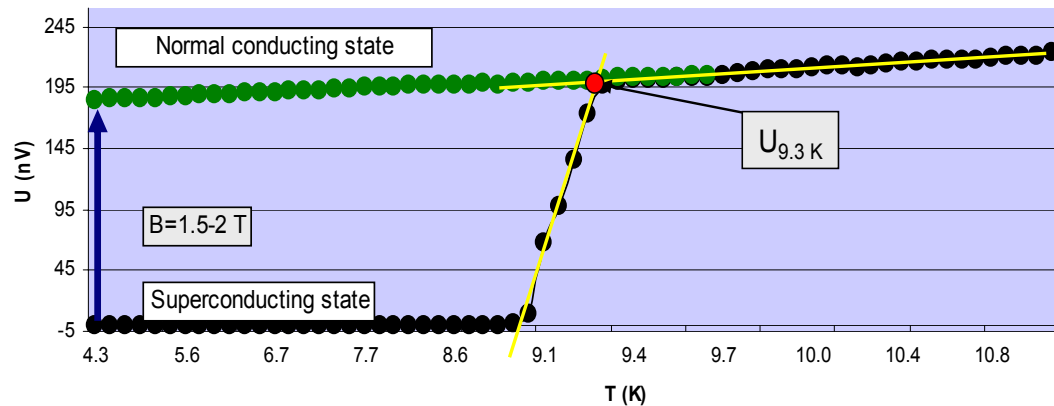


Fig. 5. DC-method: extrapolation of $U(T)$ curve of Nb300

In some of the companies producing Nb and in a few scientific centers a similar approach in determining RRR is used [11, 12, 14, 18, 19].

The scientific group at CEA Saclay (France) proposed another way of extrapolation: the RRR -value is calculated from the relation (R_{300K}/R_{0K}) taking into account that the phonon contribution at $T_C=9.3$ K cannot be neglected because of its temperature dependence. In this case it is calculated from measurements done above the critical temperature and then extrapolated to $T=0$ K using the simplified law: $R_{0K} = R(T) - \alpha R_{300K} T^3$. This expression is valid for many metals and in the case of Nb $\alpha = 5.10^{-7} \text{ K}^{-3}$ [18].

The scientific group at Frascati (Italy) proposed the RRR definition as a ratio of the resistivity at room temperature and the resistivity at 9.3 K with subsequent extrapolation to 4.2 K [19]. The results obtained by this method agree well with the measurements performed at DESY. The same method for RRR measuring is used by Fa. Niowave Inc. [20].

Accuracy estimation: as already described in section 3.1, an additional error comes from the procedure of the $\rho(T)$ curve extrapolation. The accuracy of $\rho(T)$ extrapolation itself depends on the temperature and voltage drop determination. Appearance of thermoelectric voltages and amplifier drifts can also be minimized by a change of the current of polarity.

The accuracy estimation is similar to the one described in section 3.1 and is also here in the range of 2-3%. It is worthwhile to use the isothermal measurements cell.

3.3. DC-method: RRR determination by extrapolation of $\rho(B)$ curve

In order to measure the residual resistivity at 4.2 K (below T_C), the superconducting state could be suppressed by a magnetic field with a strength $B > B_{c2}$. For Nb, $B_{c2} \sim 300$ mT [3, 21].

The realization of this method is as follows: the Nb sample is completely immersed in liquid helium ($T=4.2$ K). A sufficiently high external magnetic field is

applied and the curve $\rho(B)$ is obtained. The applied magnetic field is parallel to the sample axis and to the current flow direction.

In this case the magnetic term ρ_m of electrical resistivity (see equation 2) has to be taken into account. Generally the magnetoresistivity of paramagnetic metal is given as

$$\rho_m = \frac{\hbar k_f}{\Delta \pi Z} \left(\frac{m^* \Gamma}{e \hbar} \right) (g_j - 1) J(J + 1) \quad (12)$$

where Z is the number of conduction electrons per unit volume, m^* -the effective electron mass, g_j -the Lande factor, J -the quantum number of full mechanical moment, Γ -the integral of exchange interaction [6]. Taking into account that the resistivity without magnetic field depends on the relaxation time τ as in [22, 23] $\rho_{res} = m^* / ne^2 \tau$, the fractional increase of the resistivity in the magnetic field of a metal can be described as a universal function according to Kohler's rule:

$$\frac{\Delta \rho}{\rho} = F \left(\frac{H}{\rho_0} \frac{m^*}{ne^2} \right) \quad (13)$$

where e and n are, respectively, the charge and concentration of electrons.

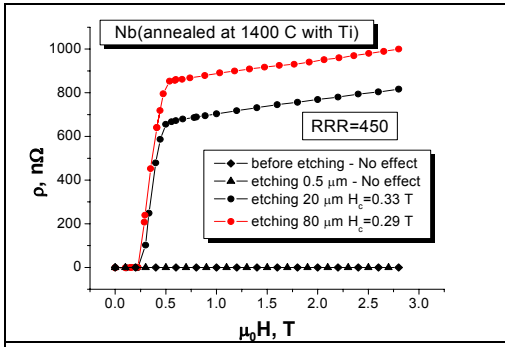


FIG. 6. Niobium resistivity at 4.2K dependence $\rho(B)$ on annealed Nb sample with $RRR=450$

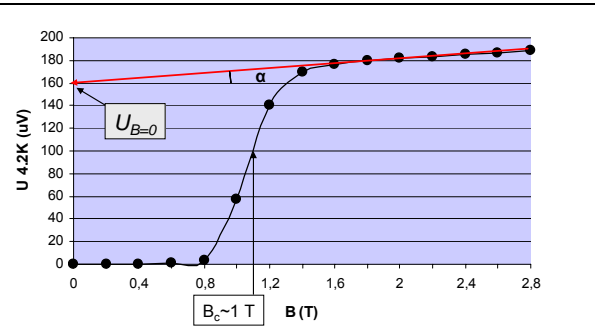


FIG. 7. RRR determination by the field extrapolation method

DESY experiments have shown (see Fig. 6) that the applied magnetic field does not penetrate into the niobium samples even up to 2.8 Tesla of the external magnetic field if the surface of the sample is not sufficiently chemically treated. Only removal of up to 50 μm of the surface layer usually results in the sharp transition from superconducting to normal conducting state.

For a correct estimation of the RRR , the magnetoresistivity term of ρ has to be excluded. This can be done by extrapolation of the curve $U_{4.2K}(B)$ to zero magnetic field. The dependence of magnetoresistivity on the magnetic field for niobium (Fig. 7) appears to be linear. A more detailed investigation of the resistivity behavior at magnetic fields above the transition jump shows that the magnetoresistivity coefficient α is slightly dependent on the RRR value and on the thickness of the layer removed by etching. The variation of the magnetoresistivity coefficient observed by DESY is between 2.8×10^{-11} and $3.1 \times 10^{-11} \Omega\text{m}/\text{T}$. Within a degree of uncertainty of the measurement instruments, α could be assumed to be the same. Some smaller dependence of magnetoresistivity at a low magnetic field was observed by Goodrich at $T > T_c$ [10]. The magnetic field produced by the current transported through the sample should be taken into consideration. In Goodrich's report, a transport current of 2A may cause a shift of the penetration field by up to 0.2 T. Considering this factor, it

would be realistic to extrapolate the resistivity to zero field by linear matching beginning with the magnetic field closest to 3T.

It can be concluded that magnetoresistivity is almost not dependent on RRR for high purity niobium and could be assumed to be the same. Therefore, the same magnetoresistivity coefficient can be used for all specimens of high purity niobium in the first approach. This means that the measurement can be done at a fix magnetic field that is high enough to keep the specimen in a normal conducting state (2T normally). After that, the magnetoresistivity $\alpha \cdot B$ can be subtracted. In practice, two voltages are measured: U_{300K} at room temperature and $U_{4.2K}$ in liquid helium. The RRR is calculated as:

$$RRR = 1 / \left(\frac{U_{4.2K}}{U_{300K}} - \frac{\alpha \cdot B}{\rho_{300K}} \right) \quad (14)$$

Where $\rho_{300K} = 1.45 \times 10^{-7} \Omega m$ [9, 16], $\alpha \approx 2.93 \times 10^{-11} \Omega m / T$ (the average value of 4 specimens); for the magnetic field of 2T

$$RRR = 1 / \left(\frac{U_{4.2K}}{U_{300K}} - 4.07 \cdot 10^{-4} \right) (B=2T) \quad (15)$$

This formula can be used for quick RRR evaluation. To get better accuracy, the extrapolation method has to be used.

Accuracy estimation: The advantage of this method is based on its high reproducibility and high accuracy. Since the sample is totally immersed in liquid helium, the instability of temperature along the sample is negligible and does not play a role. By averaging many points, the drop voltage detection can be very precise. Samples with a contaminated surface layer show different critical fields at superconducting jumps (0.3-1.5 T); nevertheless the error related to the extrapolation procedure is not high due to nearly the same slope of the curve $\rho(B)$. Based on DESY parameters the systematic error from instruments can be estimated as 1-2%.

Our colleagues at Cornell University [24] apply a low frequency AC technique for RRR measurement using a method similar to the $\rho(B)$ method described above. The difference is that, in contrast to DC measurements, a lock-in amplifier is used to measure the voltage drop along the sample. This technique gives a higher accuracy for the assessment of voltages and eliminates the voltage offset common in DC measurement, produced upon contact with different metals. The drive signal to the sample is typically a 30 Hz, 5 Ampere sinusoid with demodulation of the sense signal followed by a 0.1-1 Hz low pass filter (see Fig. 8).

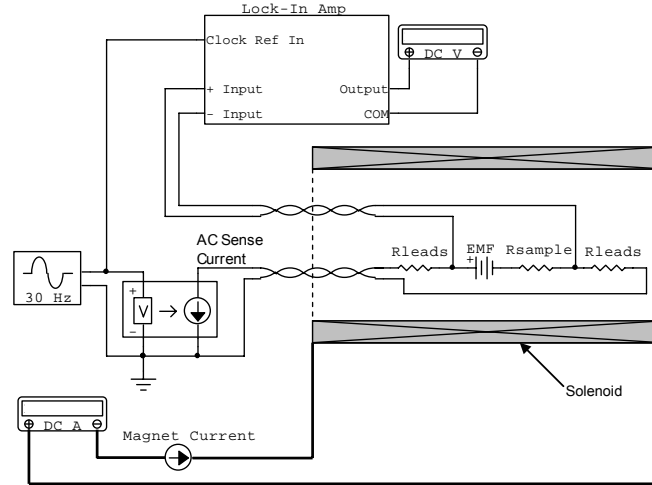


FIG. 8. Setup of the lock-in amplifier technique for accurate measurement of the low sample voltages using the $\rho(B)$ method for RRR measurement [24].

3.4. AC-methods of nondestructive RRR measurement

During cavity fabrication Nb goes through multiple stages of treatments (annealing, chemical and electrochemical polishing, electron beam welding, centrifugal barrel polishing etc.). At each stage the purity of the Nb can be significantly diminished.

For the control of purity at such stages a non-destructive RRR eddy current (AC) measurement system has been developed at DESY. It is designed for controlling RRR directly on the surface of the superconducting resonators.

In the AC case, the electrical resistivity (Eq. 2) includes one more term - ρ_{sf} . The term ρ_{sf} refers to the surface resistance that describes the surface energy dissipation for both the normal and superconducting states.

In a good conductor in the normal state the electromagnetic fields are attenuated exponentially by the distance from the surface (Fig. 9). ρ_{sf} in this case:

$$\rho_{sf} = 1/\sigma\delta \quad (16)$$

where: σ is conductivity, μ - permeability, δ - skin penetration depth:

$$\delta = 1/\sqrt{\pi\mu\sigma f} \quad (17)$$

The high frequency surface resistance of metals in the superconducting state determined from Maxwell's and London equations is given as follows:

$$\rho_{sf} \propto \omega^2 \frac{n_n}{n_s^{3/2}} \quad (18)$$

The superconducting state surface resistance is expected to drop quickly towards zero as the temperature drops below T_C because the number of superconducting electrons n_s increases rapidly while the number of normal conducting electrons n_n decreases [25, 26, 27]. The term ρ_{sf} can be neglected in practical implementations (see below) comparable to resistance caused by impurity scattering. It is well-known that when a

normal conducting metal is placed in an AC magnetic field with the frequency f , an eddy current will be induced in the metal (Fig. 9).

The detection and measurement of the magnetic fields, generated by eddy current, allow for obtaining contact-less information about the conductive properties of materials. The measurement probe consists of a primary coil for establishing the AC magnetic field, a pick up coil for detecting the eddy current, and a backing coil for

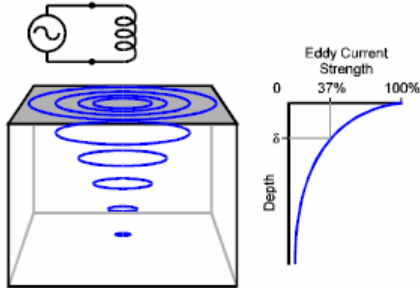


FIG. 9. The induced eddy current in the metal under an AC magnetic field

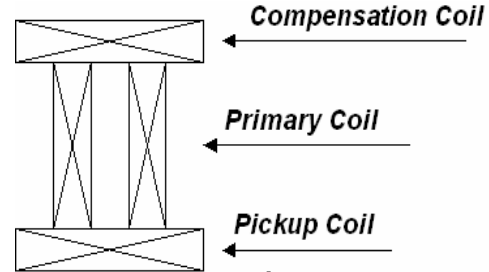


FIG. 10. Schema of the probe for RRR AC measurement

compensation of the signal induced by the primary coil (Fig. 10).

The primary coil is a small solenoid magnet with ca. 50 windings. The pickup coil is a one-layer pancake coil (Fig. 11).

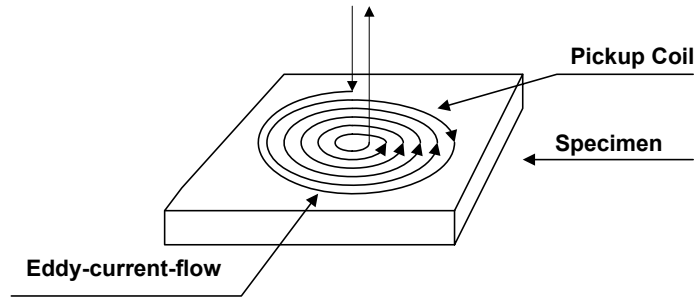


FIG. 11. One-layer pancake-shape coil

The backing coil has the same shape as the pickup coil but with an oppositely induced voltage direction for eliminating the signal induced by the primary coil in the pickup coil. Similar ideas with pick up and backing coils have been used for RRR measurements at KEK by M. Wake and K. Saito [28].

Considering the fact that the mutual induction between primary coil and sample can be modelled as a transformer, an electric potential in the sample will be produced as:

$$\vec{E}_s = M \cdot \frac{d\vec{I}_{pr}}{dt} \quad (19)$$

The eddy current is

$$\vec{I}_s = \vec{E}_s / R_s = \frac{M}{R_s + jX_s} \cdot \frac{d\vec{I}_{pr}}{dt} \quad (20)$$

where M is the mutual inductance, R_s -the real part of the resistance, X_s -the imaginary part of the resistance, I_{pr} -the current through the primary coil, t -time.

It is not so easy to express quantitatively the relationship between the eddy current and the sample resistivity since this depends on the probe structure, the sample shape, the distance between coil and sample etc. A relative method based on the relationship

between pick-up voltage jump at T_C and RRR is applied. One measures the temperature dependence of the pick-up voltage (Fig. 12).

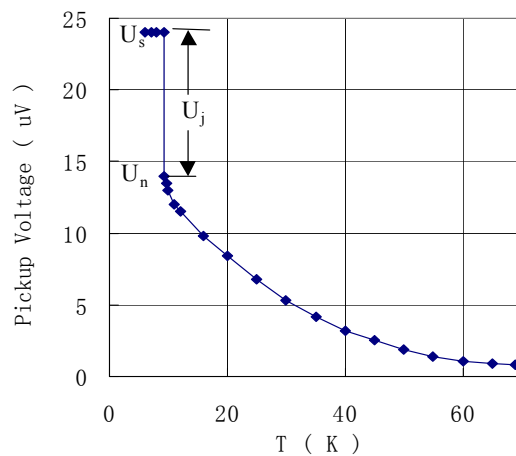


FIG. 12. Pickup voltage vs. temperature. U_s and U_n are the voltage in superconducting and normal conducting state respectively

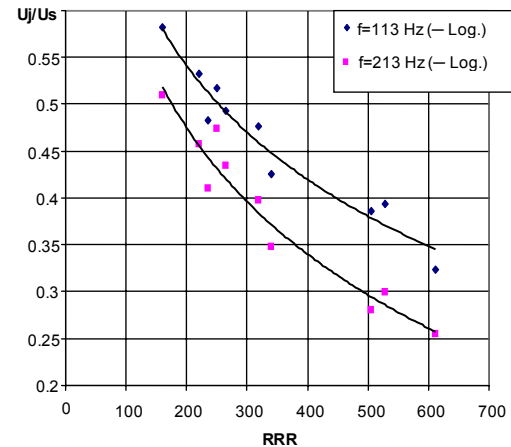


FIG. 13. Calibration curves of U_j/U_s vs. RRR for two different frequencies

RRR can be estimated by looking at the value of the superconducting jump U_j , using previously created calibration curves of U_j/U_s versus RRR (see Fig. 13).

Accuracy estimation: Two main factors influence the measurement accuracy. At higher RRR -values (500 - 600) the slope of the calibration curve U_j/U_s vs. RRR is less steep, which reduces the accuracy of RRR measurement in this area.

The other important factor is the temperature homogeneity of the cavity close to T_C , needed for a clearly expressed superconducting jump. The temperature deviation during cool-down should not exceed 0.1K. The superconducting jump is sufficiently expressed for temperature identification with an error less than 0.2K. Therefore, the error for a RRR value around 300 due to cool-down or warm-up can be well controlled within 3%.

The systematic error coming from instruments and current sources can be controlled within 1%. The pickup cables have to be twisted for minimizing parasitic noise.

One important item affecting the accuracy is the distance between the probe and the cavity surface. The distance variation can be indicated by U_s . For the same coil and the same primary AC current, U_s is strongly dependent on the distance variation. The measured RRR dependence on the distance d between probe and the niobium sample is shown in Fig. 14. It can be seen that the deviation of RRR can be within 5% for a distance deviation between probe and cavity wall smaller than 0.2 mm. Careful probe installations allow for reaching the contact quality of this level or even better.

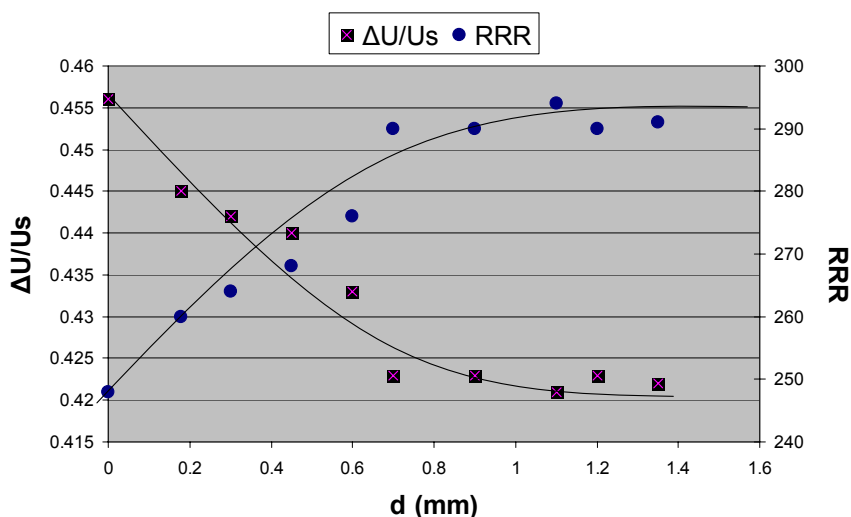


FIG. 14. Influence of distance between probe and sample surface on RRR measurement

Considering all above-mentioned aspects, the final relative RRR error can be estimated as 10% for $RRR=300$ and in the range of 15% for $RRR=600$.

It has to be mentioned that the meaning of RRR measured by the 4-point and by the eddy current method has some differences. The RRR value measured by 4-point method is the average value of a bulk sample, while eddy current indicates the RRR of a layer close to the surface area. The thickness of this layer depends on the applied frequency and, for DESY equipment, is approximately 500 μm .

A similar AC inductive method for RRR determination was developed by the scientific group of CEA Saclay [16, 29].

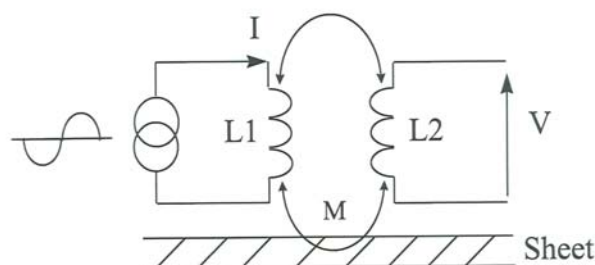


FIG. 15. Electronic set-up of inductive method

The idea of this method is changing the mutual inductance of a pair of coils touching the niobium sheet (Fig. 15). A known AC current is introduced in the primary coil $L1$. The AC voltage V induced in the secondary coil $L2$ is measured.

In order to minimize systematic errors, V is measured both with the niobium sheet in the normal conducting state at 10 K (V_{10K}) and in the superconducting state (V_s). The ratio V_{10K}/V_s is plotted as a function of frequency (Fig. 16).

In normal conducting state, the eddy current induced in the niobium penetrates on a skin depth (Eq. 17). At high frequencies δ tends to zero. In this case the electromagnetic wave is totally reflected. The ratio V_{10K}/V_S tends to reach saturation.

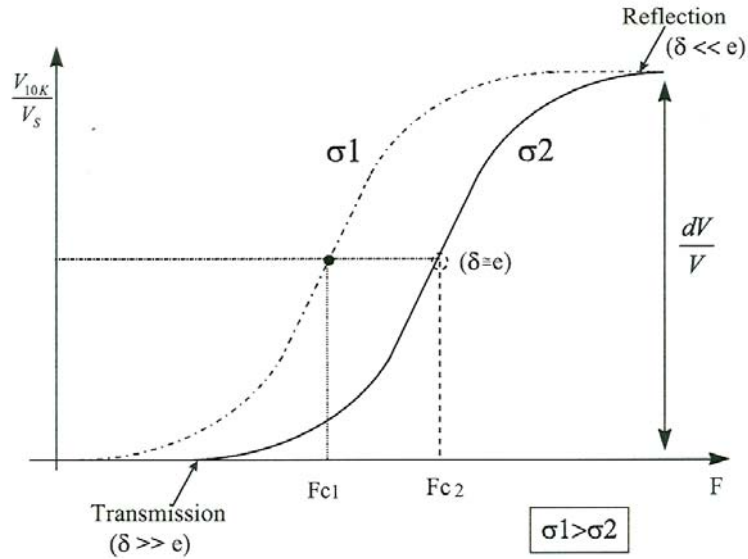


FIG. 16. Plot of ratio V_{10K}/V_S versus frequency (F in log scale)

At very low frequencies the sheet becomes transparent to the AC electromagnetic field because the penetration depth becomes larger than the niobium sheet thickness. The ratio V_{10K}/V_S tends to a constant value.

Between these two extreme points, the curve $V_{10K}/V_S(f)$ has an inflection for frequency f_c where the penetration depth δ is of the order of the sheet thickness t . For given coil geometry and sheet thickness, the curve $V_{10K}/V_S(f)$ depends only on the material RRR . Taking two metal sheets of equal thickness with resistivity ρ_1 and ρ_2 respectively, the penetration of the magnetic field, as it can be seen from Eq. 17 is the same in both sheets for two frequencies f_1 and f_2 as $f_1/f_2 = \rho_1/\rho_2$. More generally, these two sheets have similar $V_{10K}/V_S(f)$ curves: $V_{10K}/V_S(f)$ (metal 1) = $V_{10K}/V_S(f)$ (metal 2). Thus obtaining $V_{10K}/V_S(f)$ curves for both metals can give the ratio ρ_1/ρ_2 . In this case only one single metal sheet can be measured at 300 K and at 10 K. The frequency ratio between the curves $V_n/V_S(f)$ at $T=300K$ and $T=10K$ gives the ratio: ρ_{300K}/ρ_{10K} . Using the formula

$$\frac{\rho(T)}{\rho_{300K}} = A + BT^3 \quad (21)$$

and obtaining the $\rho_{4.2K}$ by extrapolation, the RRR is defined as $RRR = \rho_{300K} / \rho_{4.2K}$

The relative variation of resistivity $\rho_n(T)$ at ca. 10K varies with temperature as follows [29]:

$$\frac{d\rho_n}{\rho_n} = -\frac{dRRR}{RRR} = 1.2 \cdot 10^{-6} \cdot T^2 \cdot RRR \cdot dT \quad (22)$$

Three sources (temperature uncertainty, systematic errors and reproducibility) have been taken into account for error estimation. The overall relative precision of the RRR measurements was defined as 5% for RRR -values of 200. This was confirmed by comparison with results of 4-point measurements.

A sophisticated method of surface RRR measurement of high-purity superconducting Nb cavities is proposed by G. Ciovati at Jefferson Lab [30]. According to the author the RRR of the surface of a complete niobium superconducting cavity can be obtained from the quality factor Q_0 of the TM_{010} mode at 10 K and 300 K [30]. The loaded quality factor Q_L is directly measured. $Q_0(T)$ is then calculated from

$$Q_0(T) = Q_L(T)(1 + \beta_1 + \beta_2) \quad (23)$$

where β_1 and β_2 are the coupling coefficients of the input and output probes, obtained by standard RF measurements [3].

The surface resistance $R_s(T)$ of the cavity can be calculated from

$$R_s(T) = G/Q_0(T) \quad (24)$$

where G is the geometry factor which depends only on the cavity shape and is known for each shape (calculated with a computer code like SUPERFISH). Fig. 17 shows the surface resistance as a function of temperature, between 10 K and 285 K, for a single-cell cavity at 1.47 GHz [30].

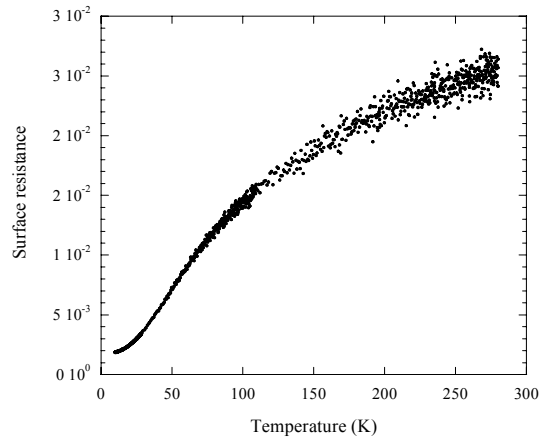


FIG. 17. Surface resistance of elliptical 1.47 GHz niobium cavity between 10 K and 285 K.

A computer code which calculates the surface impedance of normal conductors at frequency f_0 and temperature T is then used to obtain the DC resistivity $\rho(T)$ from the surface resistance $R_s(T)$ [31]. The input material parameters for the code are the electron density ($\sim 8.1 \times 10^{28}$ 1/m³ for Nb) and the product $\ell\rho$ ($\sim 6 \times 10^{-16}$ Ωm^2 for Nb), where ℓ is the electrons' mean free path. Using the RRR value defined for example by $RRR = \rho(300\text{K})/\rho(10\text{K})$ the RRR can be easily determined. The resistivity values obtained with this technique represent a depth of the order of the skin depth.

The typical experimental error is 10%, mainly due to the uncertainty in the measurement of Q_L .

4. Conclusions

The above-described DC and AC RRR measurement methods comprise different approaches to the purity control of niobium on samples and bulk niobium cavity in-situ.

The DC-methods based on the similar principles show comparable results for the RRR -values. The common advantage of DC-methods is the relatively high accuracy in measuring RRR and the reproducibility. The DC-methods are destructive methods and

therefore can be used only for quality control of niobium material before start of cavity fabrication.

The most preferable procedure for *RRR* evaluation used not only at DESY but also in many other laboratories [11, 12, 18, 19], seems to be the DC method with extrapolation of the $\rho(T)$ curve to 4.2 K. Relatively high accuracy of the method can be reached by precisely measuring the $\rho(T)$ curve. High temperature stability can be provided by using an isothermal measurement cell. In this case accurate measurement of the transition temperature T_C is possible, which gives additional information about purity, because T_C is sensitive to the content of impurities (see for example [32]).

The DC-method that defines *RRR* as ratio $R(300K)/R(T_C)$ has similar advantages and disadvantages as the method using the extrapolation of $\rho(T)$ curve to 4.2 K. It should be noted that in this case the *RRR* values are ca. 8-10% smaller compared to *RRR* determined on the basis of the common *RRR* definition of $RRR=R(300K)/R(4.2K)$.

The DC method for *RRR* evaluation based on the suppression of the superconducting behavior of niobium by an external magnetic field allows performance of quick measurements with high accuracy. At the same time this method requires a magnetic system applied at low temperature with high uniformity of the field. The samples prepared for this method should be sufficiently etched to ensure full penetration of the applied field into the sample. Either temperature or field extrapolation DC methods should lead to comparable results. Experience of *RRR* measurements on samples with a wide range of *RRR* verifies this.

The AC-methods performed directly on the cavity surface makes it possible to estimate the *RRR* value on a definite location of the cavity or average *RRR* value of the complete cavity as delivered by the cavity producer or after different stages of cavity preparation. Even creation of a *RRR* map of the cavity is feasible [29]. However the accuracy in *RRR* estimation by AC-methods is less than that of DC-methods.

The method of sample extraction from the niobium piece without contamination is a special issue. During sample preparation the protecting oxide layer is destroyed and contamination can occur. Several cutting methods are used at different laboratories: milling, EDM, water jet cutting, diamond saw, band saw, shearing et al. Investigation of the influence of the cutting techniques on contamination and surface morphology of high purity niobium can be found in references [33, 34].

Acknowledgements

Thanks to G. Ciovati, E. Chojnacki and J. Sears for supplying information about *RRR* measurement techniques in their labs. Many thanks to M. Tigner who initiated this paper, to P. Kneisel, H. Weise and many other DESY colleagues for helpful discussions.

References

-
- [1] W. Wasserbäch, Low-temperature thermal conductivity of plastically deformed niobium single crystal, Philosophical Magazine A, 1978, Vol.38, No.4, 401-431.
 - [2] L. P. Kadanoff, P. S. Martin, Theory of many-particle systems. II. Superconductivity, Phys. Review, 124, (1961), 670

-
- [3] H. Padamsee, J. Knobloch, and T. Hays, RF superconductivity for accelerators, J. Wiley & Sons, New York, 1998
 - [4] Physicalmetallurgy: 4th Revised and Enhanced Edition, edited by R.W. Cahn and P. Haasen, 3 volumes, 2984 pages North-Holland Amsterdam-Lausanne-New York-Oxford-Shannon-Tokyo, ISBN 0-444898-75-1 (1996)
 - [5] P.L. Rossiter, The electrical resistivity of metals and alloys, Cambridge Solid State series, Cambridge University Press, 1987
 - [6] K. N. R. Taylor, 'Intermetallic rare-earth compounds', *Advances in Physics*, 20: 87, 551 -660, 1971
 - [7] M. Hörmann, The production of high thermal conductivity niobium on a technical scale for high frequency superconductors, Heraeus, Hanau (1988).
 - [8] Ralf W. Röth, Grenzfeldstärken und Anomale Verlustmechanismen in Supraleitenden Beschleunigungsresonatoren aus Niob, Dissertation, Wuppertal, 1993 (WUB-DIS 92-12)
 - [9] K. K. Schulze, "Preparation and characterization of ultra-high-purity niobium," *J. Met.*, vol. 33, pp. 33–41, 1981
 - [10] L. F. Goodrich, T. C. Stauffer, J. D. Splett, D. F. Vecchia, "Measuring residual resistivity ratio of high-purity Nb", *Advances in Cryogenic Engineering Materials*, Vol. 50A, pp. 41-48, 2004
 - [11] P. Bauer, T. Berenc, C. Boffo, M. Foley, M. Kuchnir, Y. Tereshkin, T. Wokas, RRR measurements on niobium for superconducting RF cavities at FERMILAB, Proceedings of 11th workshop on RF superconductivity (SRF-2003), 8-12 Sept. 2003, Lübeck/Travemünde, Germany
 - [12] H. Umezawa, Impurities analysis of high purity niobium in industrial production, *Matériaux & Techniques*, № 7-8-9, 2003
 - [13] Technical specification for large crystal niobium discs applied for the fabrication of 1.3 GHz superconducting cavities, W. Singer, DESY, 2008
 - [14] P. Bauer, C. Antoine, Technical specification for high rrr grade niobium sheet and rod for use in superconducting cavities, Fermilab, March 21, 2006
 - [15] W. Singer, D. Proch, The eddy current method for RRR measurement of superconducting materials, SRF workshop SACLAY, 1995
 - [16] M. Bolore, B. Bonin, Y. Boudigou, S. Heuveline, E. Jacques, S. Jätdane, F. Koechlin, H. Safa, "A New Inductive Method for Measuring the RRR-value of Niobium", *Proc. of the 7th Workshop on RF Superconductivity*, CEA-Saclay, Gifsur-Yvette, France (1995), p541-545.
 - [17] K.-H. Berthel, "Beiträge zur Supraleitung, Elektronenstruktur und zum elektrischen Widerstand von Hochreinem Niob", Dissertation, Technische Universität Dresden, 1976
 - [18] C. Z. Antoine, Analysis of impurities in high purity niobium: surface vs bulk, *Matériaux & Techniques*, № 7-8, 2003
 - [19] G. Fuga, M. Minestrini, R. Sorchetti, RRR measurements test facility, Pr. Com., INFN-LNF, Frascati, Italy
 - [20] T. Grimm, Niowave, Inc. 1012 N Walnut St. Lansing, MI 48906 USA
 - [21] P. Schmüser, Basic principles of RF superconductivity and superconducting cavities, Workshop 'Pushing the Limits of RF Superconductivity', September 22-24, Argon National Laboratory, USA, 2004
 - [22] N. Luo, G. H. Miley, Kohler's rule and relaxation rates in high- T_C superconductors, *Physica C* 371, 259-269, 2002

-
- [23] G. W. Webb, “Low temperature electrical resistivity of pure niobium”, *Phys. Rev.* 181(3), pp1127-1135, 1969
- [24] E. Chojnacki, J. Sears, Private communication, 2008
- [25] J. M. Pierce, In *Methods of Experimental Physics*, Vol. 11, ed. R. V. Coleman, Academic Press, NY, p. 541, 1974
- [26] W. H. Hartwig, C. Passow, in *Applied Superconductivity*, Vol. 2, ed. Newhouse, Academic Press, NY, 1975
- [27] J. D. Jackson, *Classical electrodynamics*, 2nd edition, John Willey and Sons, NY, 1975
- [28] M. Wake, K. Saito, *RRR measurement of superconducting cavity materials using eddy current*, Proc. of the 7th Workshop on RF Superconductivity, CEA-Saclay, Gif-sur-Yvette, France (1995)
- [29] H. Safa, Y. Boudigou, E. Jacques, J. Klein, S. Jaidane, M. Boloré, *RRR mapping of niobium superconducting cavities by magnetometric method*, 8th Workshop on RF Superconductivity, Abano Terme (Padova), 4-10 October, 1997
- [30] G. Ciovati, “Investigation of the superconducting properties of niobium radio-frequency cavities”, Ph.D. Dissertation, Old Dominion University, Norfolk, 2005
- [31] R. Schwab, “Program CASINOCO: Calculation of the surface impedance of normal conductors at arbitrary frequencies and temperatures”, Forschungszentrum Karlsruhe Report No. 6023, 1997
- [32] B. Fellmuth, D. Elefant, J.-I. Moench, *Investigation of superconducting transition of ultra-high-purity niobium*, *Phys. Stat. Solidi (a)*, 100, 597, 1987
- [33] C. A. Cooper, A. Wu, P. Bauer, C. Antoine, *Effect of different cutting techniques on the surface morphology and composition of niobium*. Proceedings of the Applied Superconductivity Conference (ASC 2008), USA, Chicago, 2008
- [34] W. Singer, X. Singer, H. Wen. *Influence of interstitials on properties of high purity niobium for RF cavities*, *Matériaux & Techniques*, N° 7-8-9, P.13-18, 2003